metals

MDPI

Article

Microstructure and Properties of Fine-Grained WC-10Co-0.5Cr_3C_2-1TaC-0.5Ru Prepared by Rolling Ball Milling and Low-Pressure Sintering

Yijing Huang [1,2], Ke Xiong [1,2], Qin Qin [3], Lin Yu [1,4], Lin Huang [1,2,*] and Wei Feng [1,2,*]

[1] School of Mechanical Engineering, Chengdu University, Chengdu 610106, China; huangyijing@stu.cdu.edu.cn (Y.H.); xiongke@stu.cdu.edu.cn (K.X.); yulin@stu.cdu.edu.cn (L.Y.)
[2] Sichuan Province Engineering Technology Research Center of Powder Metallurgy, Chengdu 610106, China
[3] Chengdu Jincheng College, Chengdu 611731, China; qinqin@cdjcc.edu.cn
[4] Sichuan Yiran Material Technology Co., Ltd., Chengdu 610100, China
* Correspondence: huanglin@cdu.edu.cn (L.H.); fengwei@cdu.edu.cn (W.F.)

Abstract: This study focuses on the preparation of fine-grained WC/Co composite powder using rolling ball milling and spray drying techniques. The cemented carbide composition achieved through low-pressure sintering technology was WC-10Co-0.5Cr_3C_2-1TaC-0.5Ru (wt.%). To study the effect of sintering temperature on the microstructure and mechanical properties of WC-10 wt.% cemented carbide, the microstructure and phase constituents of the material were analyzed using X-ray diffractometry and scanning electron microscopy. Additionally, the physical and mechanical properties of the material were examined. The results indicate that as the sintering temperature increased from 1390 °C to 1450 °C, the grain size of WC in the alloy increased, resulting in a slight decrease in hardness, an increase in fracture toughness, and the transverse fracture strength increasing first and then decreasing. The sintered hard alloy prepared at 1410 °C exhibited fewer pores and a uniform and fine grain size, reaching a density of 99.98%, a hardness of 91.8 HRA, a fracture strength of 3962 MPa, and a fracture toughness of 14.7 MPa·$m^{1/2}$

Keywords: cemented carbide; sintering temperature; microstructure; mechanical properties

Citation: Huang, Y.; Xiong, K.; Qin, Q.; Yu, L.; Huang, L.; Feng, W. Microstructure and Properties of Fine-Grained WC-10Co-0.5Cr_3C_2-1TaC-0.5Ru Prepared by Rolling Ball Milling and Low-Pressure Sintering. *Metals* **2023**, *13*, 1478. https://doi.org/10.3390/met13081478

Academic Editors: Emin Bayraktar and Salvatore Grasso

Received: 30 June 2023
Revised: 10 August 2023
Accepted: 15 August 2023
Published: 17 August 2023

1. Introduction

Cemented carbide is a composite material consisting of a hard refractory metal and binder metal formed by powder metallurgy and classified as a composite cermet material [1]. WC-Co cemented carbide is one of the most essential cemented carbides, composed of a WC hard phase, which contributes to wear resistance, and a Co binder phase, which contributes to toughness [2]. WC-Co cemented carbides have high hardness, wear resistance, and excellent mechanical properties. They are known as the "teeth of industry" and have become an indispensable material in people's lives [3]. Moreover, Cemented Carbide can be stably mass-produced on a large scale, which is very suitable for the technical requirements of modern advanced manufacturing technology on high-performance tool materials. It has become a hot spot of international engineering materials development and is widely used in the field of high-efficiency and high-precision cutting and processing in automobile manufacturing, aerospace, die manufacturing, electronic information, and other industries [4,5].

Modern industrial technology development has put higher requirements on high-speed and precision machining [6]. Therefore, high demands are placed on WC-Co cemented carbide's hardness, strength, and fracture toughness to maintain the tools' manufacturing quality and efficiency [7]. The mechanical properties of WC-Co cemented carbides mainly depend on the microstructure, which is closely related to the distribution and size of WC particles [8,9]. It was found that the relationship between the hardness of WC-Co and

the average distance between the grains of cemented carbide is feasible, which is related to its microstructure [10]. Among the ultra-fine cemented carbide grades, where the WC grain size is <0.5 μm, the parts exhibit high hardness, which can prevent deep penetration of abrasives and thus have high wear resistance [11].

Conventional cemented carbide due to the contradiction between hardness and toughness, it is usually difficult to obtain cemented carbide with simultaneous improvements in hardness and toughness. Therefore, the study of the co-enhancement of hardness and toughness has become a hot issue in the cemented carbide field [12–14]. Numerous studies have shown that a good combination of high hardness and high fracture toughness can be obtained by refining WC grains [15,16]. In the conventional sintering process, WC particles grow significantly after sintering at liquidus temperature for several minutes [17]. Therefore, if the sintering process is not controlled correctly, the WC particles will overgrow, affecting the alloy's mechanical properties [9]. One of the most effective methods to control WC grain growth is to add a small amount of carbide grain growth inhibitors, such as VC, Cr_3C_2, TaC, TiC, NbC, etc. [18–20]. The addition of additives can inhibit the growth of WC grain, but the inhibition mechanism is different, so the inhibition effect is different. The effects of Cr_3C_2, TaC, and Ru grain growth inhibitors on the microstructure and mechanical properties of cemented carbide have been explored through a large number of experiments. The results show that Cr_3C_2, TaC, and Ru can effectively inhibit the grain growth of WC, and the organization is more uniform so that the cemented carbide has good comprehensive mechanical properties [21–23]. Among them, Cr_3C_2 can refine the grain, enhance the hardness, transverse fracture strength, and impact toughness [24,25]. TaC can improve the red hardness of cemented carbide, and Ru can improve the fracture toughness and service life of carbide tools [22]. In this paper, WC-10Co-0.5Cr_3C_2-1TaC-0.5Ru (wt.%) cemented carbide was prepared and further studied.

WC grain growth occurs when sintering nano-WC-Co raw powder mixtures through conventional pressureless sintering, especially in the liquid state [26]. Low-pressure sintering can reduce the porosity of the alloy, improve densification, and achieve the large-scale production of high-performance cemented carbide. The low-pressure sintering process of cemented carbide requires that the mixture be pressed and shaped, then put into the sintering furnace. After dewaxing and pre-sintering, solid-phase sintering, liquid-phase sintering, and cooling processes, the porous powder compacts into a densified alloy. Only after sintering does the cemented carbide have the required structure and mechanical properties [27–30]. Many scholars have investigated the effects of different sintering processes, such as spark plasma sintering, vacuum sintering, and low-pressure sintering, on the densification and mechanical properties of cemented carbide. It was found that low-pressure sintering resulted in lower porosity, more homogeneous organization, and better mechanical properties of cemented carbide [31–33].

The phase compositions in cemented carbides are usually WC, γ, C, η. The WC phase is called the α-phase, and the bonding phase is called the γ-phase, which is a solid solution of tungsten and carbon in cobalt. In addition, when the carbon content in the alloy is too high, a free C-phase can occur; the η phase appears when the C amount is too low. The η-phase includes ternary compounds with molecular formulas Co_3W_3C, Co_6W_6C, etc. [34]. If the sintering process is not well controlled, it is easy to form a WC + γ + c three-phase structure where a graphite phase will appear in the alloy or a WC + γ + η three-phase structure where the third-phase-η phase will appear in the alloy [35]. The appearance of the η phase or the graphite phase will worsen the properties of cemented carbides and reduce their comprehensive properties, in which sintering the temperature plays a key role [36,37]. The sintering temperature has an important effect on the size and distribution of the WC grain, the porosity of the alloy structure, and the physical-mechanical properties [38–40]. Given this, this article proposes a method for preparing WC-10Co-0.5Cr_3C_2-1TaC-0.5Ru cemented carbides based on a combination of rolling ball milling and low-pressure sintering. The influence of sintering temperature on

its microstructure, physical properties, and mechanical properties was studied. It provides a theoretical basis for the practical engineering application of cemented carbide.

2. Materials and Methods

2.1. Powders Preparation

WC powder supplied by Xiamen Jinlu Special Alloy Co., Ltd. (Xiamen, China), Co powder provided by Nanjing Coldrise Cobalt Co., Ltd. (Nanjing, China), and commercially available Cr_3C_2, TaC, and Ru powders are used as raw materials. The characteristics of raw materials are summarized in Table 1.

Table 1. Characteristics of raw materials.

Material Powder	Fisher Subsieve Sizer (μm)	Purity (wt.%)	Total Carbon Content (wt.%)
WC	1.0	99.8%	6.16
Co	1.09	99.9%	-
Cr_3C_2	0.86	99.5%	13.09
TaC	1.2	99.9%	6.18
Ru	1.0	99.95%	-

WC-10 wt.% Co cemented carbides with the addition of 0.5 wt.%Cr_3C_2, 1.0 wt.% TaC, and 0.5 wt.% Ru were designed. The equipment was a tiltable rolling ball mill, and the test process was to weigh the raw materials according to the composition ratio and add 0.5 mL dispersant per kg according to the dosage. The raw powder mixture was wet ball-milled for 60 h in ethanol, and the ball-to-powder weight ratio was 5:1 [41]. In the last 2 h of grinding, 2.2 wt.% of paraffin was added as a forming agent. After ball milling, the slurry was spray-dried and granulated using a BP-25 closed-cycle spray-drying system to obtain a WC-10Co-0.5Cr_3C_2-1TaC-0.5Ru mixture. The mixture was pressed into a 24.6 mm × 8.5 mm × 7.3 mm strip using a mold, a fully automatic electric powder autoclave, and a pressure of 150 Mpa.

The low-pressure sintering process was adopted, and the sintering equipment was a degreasing and pressurized integrated furnace. A single variable, sintering temperature, was designed to be changed to study the effect of sintering temperature on the alloy organization and properties. The press billets were sintered at target temperatures (1390, 1410, 1430, and 1450 °C, labeled D1, D2, D3, and D4, respectively), a holding time of 60 min, and a holding pressure of 4.5 MPa [42].

2.2. Analysis and Characterization

The sintered samples for microstructure observation were ground and polished with diamond pastes. A DX-2500 X-ray diffractometer (XRD, Dandong Haoyuan Instrument Co., Ltd., Dandong, China) was used for phase analysis. Cemented carbide porosity was measured using an OLYMPUS inverted metallographic microscope GX51 according to ISO 4505. The microstructure and composition of the samples were analyzed by an FEIInspectF50 field emission scanning electron microscope (SEM, FEI Company, Hillsboro, OR, USA) and an energy dispersive spectrometer. For SEM imaging of the surface of the polished samples, the image processing software Image-J (public image processing software based on Java) was used to measure WC grains via the linear intercept method (ASTM-E112-13) to calculate the average grain size and grain cumulative distribution curve of each sample. The density of the samples was measured with Archimedes' principle (ASTMB962). The ZS-II force coercive meter and the YSK-III cobalt magnetic saturation induction tester were used to determine the coercivity force and magnetic saturation, respectively (ASTMB887, B886). The hardness value HRA of cemented carbide was measured using an HRS-150 Rockwell hardness tester (Shanghai Juihui Instrument Manufacturing Co., Ltd., Shanghai, China) with a loading of 588.4 N, which complied with ASTM B294. The specimens' transverse rupture strength (TRS) was tested by three-point bending according to ASTM B406.

Fracture toughness (K_{IC}) was calculated with the Palmqvist equation based on the crack length [43]. The average TRS, hardness, and fracture toughness values were obtained from at least five measurements.

3. Results and Discussion

3.1. Phase Formation

Figure 1 shows the XRD patterns of the powder mixture after ball milling and WC-10Co-0.5Cr_3C_2-1TaC-0.5Ru cemented carbide under different sintering temperatures. As can be seen in Figure 1, all samples were composed of WC and Co phases. No graphite phase or η phase was observed in all sintered samples. In general, the carbon content greatly influences the properties of sintered WC-Co cemented carbide [44]. If the atomic weight percentage (W:C) is less than 1, carbon precipitates as graphite; conversely, if it is greater than 1, it tends to produce the η-phase in the microstructure (Co_3W_3C and Co_6W_6C) [45]. These phases impair the mechanical properties of cemented carbides [46]. It has been shown that phases such as W_2C, Co_3W_3C, and Co_6W_6C appear during the sintering process of cemented carbide. When the sintering temperature reaches a certain value, these phases disappear entirely, and only WC and Co phases are detected [47]. As shown in Figure 1, after sintering at 1390 °C, no η phase or graphite phase unfavorable to the cemented carbide was found, so it was confirmed that the WC-Co cemented carbide had been entirely sintered. Moreover, we did not observe significant differences in the increase in sintering temperature. In addition, due to the relatively small contents of Cr_3C_2, TaC, and Ru, no peaks were observed in any alloy.

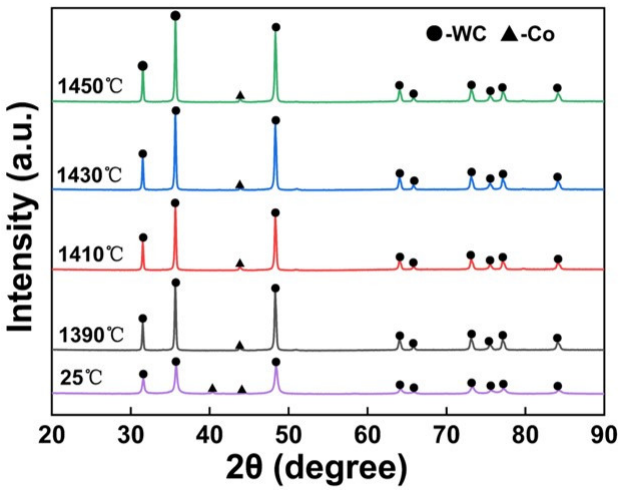

Figure 1. XRD patterns of WC-10Co-0.5Cr_3C_2-1TaC-0.5Ru powders and sintered samples at different temperatures (1390–1410 °C).

Figure 2 shows SEM images of WC, Co, Cr_3C_2, TaC, and Ru powders. It can be observed that the WC is irregularly elliptical and slightly agglomerated. The surfaces of Co, Cr_3C_2, TaC, and Ru powders are irregularly shaped and slightly agglomerated. Figure 3 shows the SEM image and particle size distribution of WC-10Co-0.5Cr_3C_2-1TaC-0.5Ru composite powder. It can be seen that the crystallinity of the powder is good, the particle size of the composite powder is fine, and the distribution is uniform. The neck formation between the WC grains and the agglomerate particles is formed. This is because, in the ball milling process, the powder is constantly crushed and cold-welded under the action of strong impact and shear forces so that the powder size is continuously reduced; with the extension of the ball milling time, the cold welding and fracture of material particles continue to deepen, and the material is constantly refined and uniform so that a large amount of surface energy, grain boundary energy, and distortion energy generated in the ball milling process through the agglomeration of grains is partially released [48]. According to the X-ray diffraction tests shown in Figure 1, the main phases of the composite

powder are the WC and Co phases. From the composite powder particle size distribution graph shown in Figure 3, it can be seen that the particle size distribution of the powder is narrow. The particle size distribution at about 0.72 μm appears to be a trailing phenomenon, which indicates that ball milling cannot uniformly crush the agglomerates.

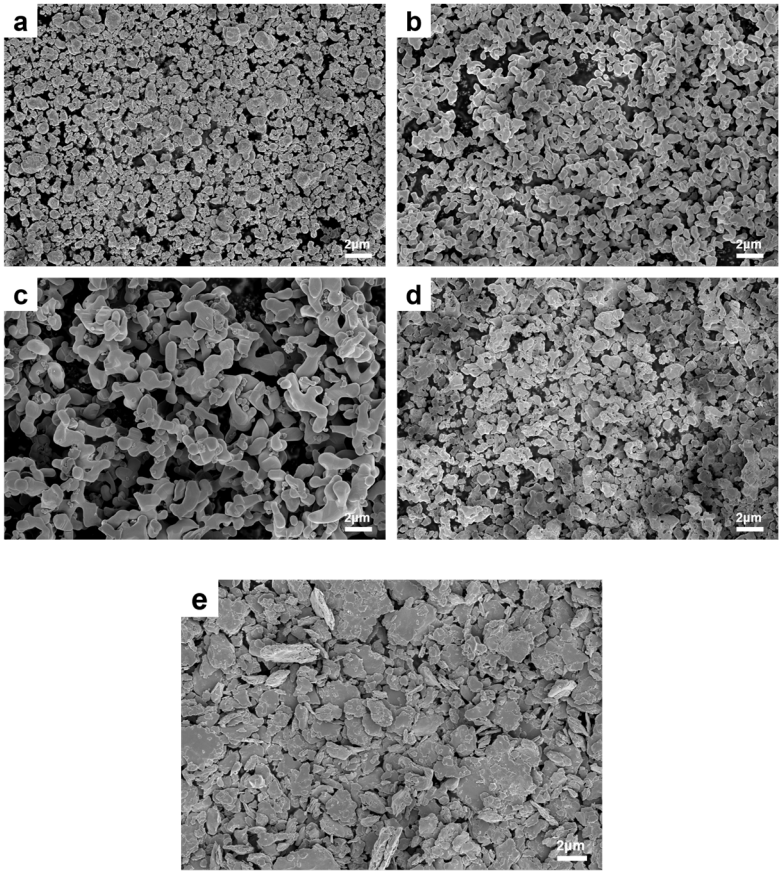

Figure 2. Scanning electron microscopy (SEM) images of (**a**) WC; (**b**) Co; (**c**) Cr_3C_2; (**d**) TaC; and (**e**) Ru raw materials.

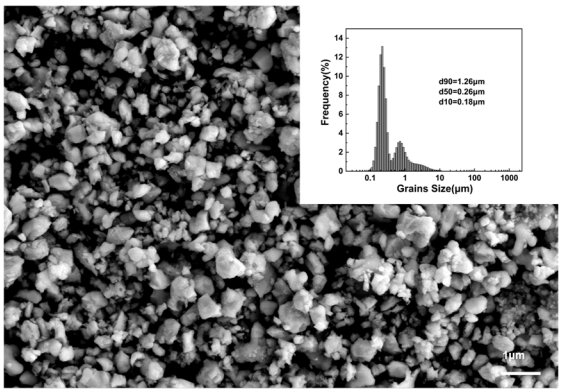

Figure 3. BSE-SEM micrographs of WC-10Co-0.5Cr_3C_2-1TaC-0.5Ru composite powders. Inset: Particle size distribution of composite powder.

3.2. Microstructure

Figure 4 shows low-magnification microstructure porosity photographs of sintered samples measured under a metallurgical microscope. Observe the polished surface and compare it with standard pictures to determine the porosity grade. All sintered samples were free of decarburized and carburized phase defects, with no large pores and only a

few tiny pores. The size of the pores is less than 10 μm, which is classified as class A pores, some of which have been circled in Figure 4a. According to the porosity judgment standard for hard alloy [49], the characteristics of the polished surface of sintered samples are presented in Table 2. The sintered sample shown in Figure 4a has the highest number of pores with a porosity of A04B00C00. This is because the sintering temperature is insufficient, and therefore there is not enough liquid phase in the alloy, resulting in some pores not being filled. Thus, micropores were formed after sintering cooling. The decrease in porosity in the sintered samples shown in Figure 4b–d indicates better densification with increasing temperature.

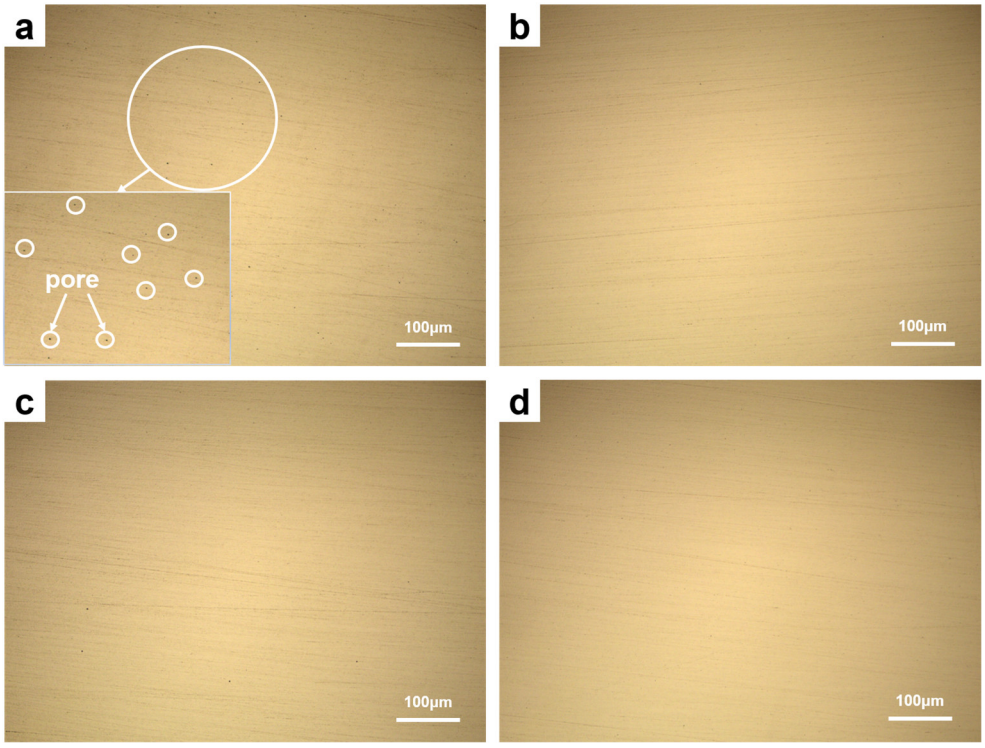

Figure 4. Porosity of WC-10Co-0.5Cr_3C_2-1TaC-0.5Ru cemented carbide at different sintering temperatures: (**a**) 1390 °C, (**b**) 1410 °C, (**c**) 1430 °C, and (**d**) 1450 °C.

Table 2. Porosity and uncombined carbon analysis (porosity: A, B; uncombined carbon: C).

Alloy	Porosity		Uncombined Carbon
	A	B	C
D1	A04	B00	C00
D2	A02	B00	C00
D3	A02	B00	C00
D4	A02	B00	C00

Figure 5 represents the elemental mapping of the WC-10Co-0.5Cr_3C_2-1TaC-0.5Ru cemented carbide. The element map provides information about the distribution of each element in the alloy. All elements are uniformly distributed in the region, and the alloy has no element segregation phenomenon. The light gray phase is WC, and the black phase is Co. At the same time, it can be seen from the diagram that Cr, Ta, and Ru elements are evenly distributed.

The microstructure of WC-10Co-0.5Cr_3C_2-1TaC-0.5Ru cemented carbides with different sintering temperatures was observed using backscattered electron mode in the SEM, as shown in Figure 6, where the bright area represents WC phases and the dark area represents Co phases. The WC particles are irregular polygons, and the Co phase is evenly

distributed in the alloys. It can be observed that most WC grains distributed in the binder Co dispersedly, while a few were adjacent to each other; most of them grew normally, while a few merged, leading to abnormal grain growth [50]. As shown in Figure 6a–d, the WC particles grow significantly with increasing sintering temperature. This is because the higher sintering temperature generates more thermal energy, which provides a greater driving force for the Co and dissolution-precipitation processes [51].

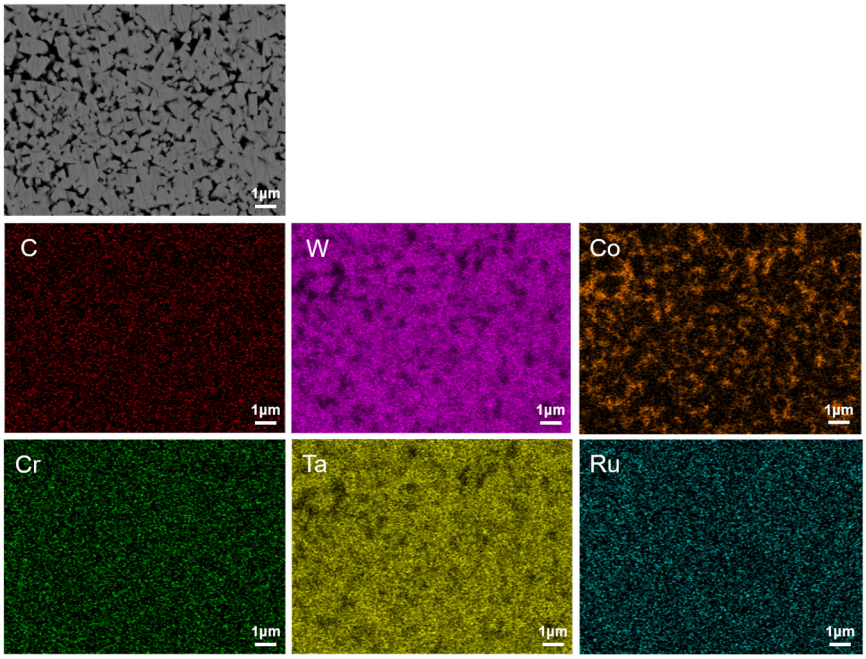

Figure 5. SEM elemental mapping of WC-10Co-0.5Cr_3C_2-1TaC-0.5Ru cemented carbide showing C (red), W (purple), Co (orange), Cr (green), Ta (yellow), and Ru (blue).

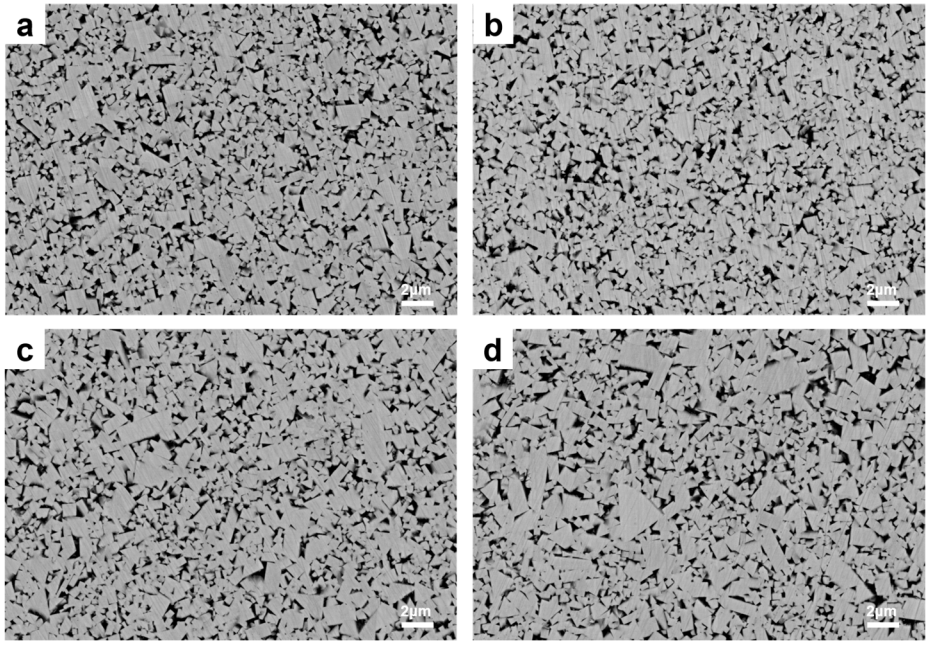

Figure 6. BSE-SEM micrograph of WC-10Co-0.5Cr_3C_2-1TaC-0.5Ru cemented carbide at different sintering temperatures: (**a**) 1390 °C, (**b**) 1410 °C, (**c**) 1430 °C, and (**d**) 1450 °C.

According to the scanning electron microscopy images of the sintered samples shown in Figure 6, the statistical analysis of WC grains was done by Image-J software. Figure 7

shows WC's average grain size and size distribution in WC-10 wt.% Co sintered cemented carbides. It can be clearly seen in Figure 7a that the WC grain size distribution is narrow and dense. From Figure 7a−d, it can be seen that the average grain size of WC becomes larger as the sintering temperature increases, and the average grain size increases from 0.664 μm to 0.711 μm. The grain distribution becomes wider, indicating that the overall grain size becomes larger. These results are consistent with the SEM examination in Figure 6. The reason is that the increase in sintering temperature increases the amount of liquid phase, which accelerates the dissolution and precipitation of tungsten carbide and promotes WC's recrystallization and recrystallization processes, resulting in a larger overall grain size in the alloy [52]. At the same time, some of the tiny particles of WC were dissolved in liquid Co and deposited on the surface of the large particles of WC, increasing the average grain size [53].

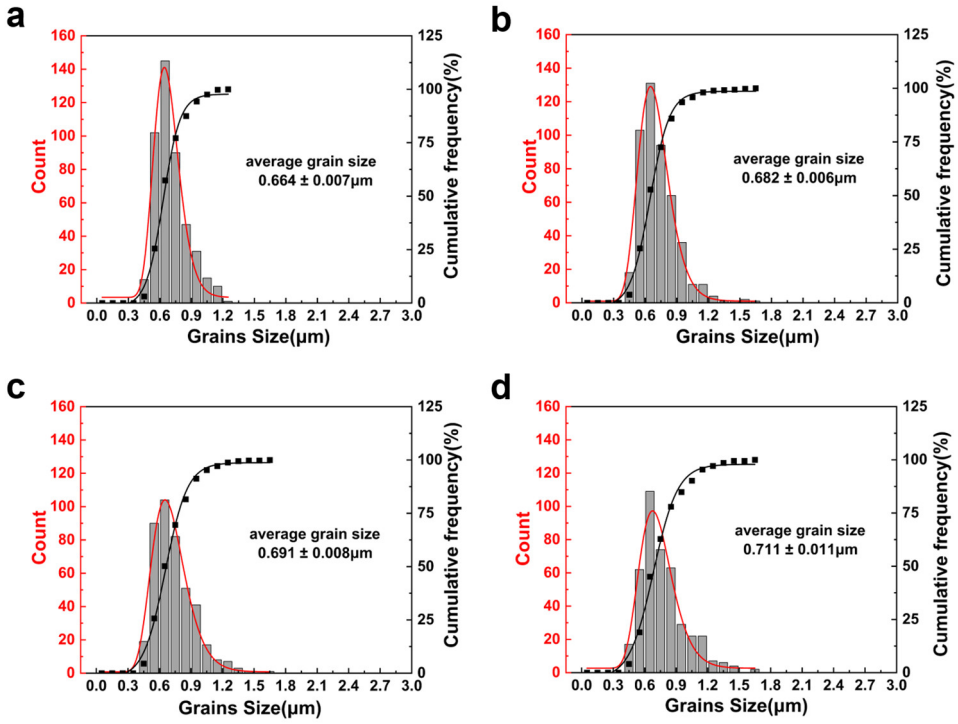

Figure 7. Grain size distribution of WC-10Co-0.5Cr_3C_2-1TaC-0.5Ru cemented carbide at different sintering temperatures: (**a**) 1390 °C, (**b**) 1410 °C, (**c**) 1430 °C, and (**d**) 1450 °C.

3.3. Physical Properties

According to the Archimedes principle, the density of each sintered sample is measured. The theoretical density of the sample is 14.413 g/cm^3 and the relative density of all samples can be calculated, as shown in Table 3. The results show that when the sintering temperature is 1390 °C, the relative density of sintered sample D1 is 99.84%, and the sample has essentially been densified. As the temperature increases, the relative density of samples D2−D4 reaches 99.98%. This indicates that the degree of densification of sample D1 is relatively low, as evidenced by the porosity detection results under the metallographic microscope shown in Figure 4. This was mainly related to the dissolution of hard-phase WC grains in Co. With the increase in temperature, the solubility of WC (there are solubility limits for W and C in liquid Co) increased, and the WC grains dissolved in Co increased. The continuous dissolution and precipitation promote further densification of the alloy. In addition, the increase in temperature also provided heat energy, increasing the activity of Co and improving its driving force [51]. Therefore, it enhances the fluidity of the liquid phase, fills the pores more fully during the sintering process, and reduces the micropores. When the alloy was densified at 1390 °C, it slightly increased the density of the sample and further increased the relative density of the alloy when the temperature was raised to

1410 °C. However, further increasing the sintering temperature results in less liquid phase being generated, and the temperature change had little effect on the relative density.

Table 3. Relative density of WC-Co cemented carbide at different ball-milling times and sintering temperatures.

Alloy	Density (g/cm^3)	Relative Density (%)
D1	14.39	99.84
D2	14.41	99.98
D3	14.41	99.98
D4	14.41	99.98

Figure 8 shows the effect of sintering temperature on the coercivity and magnetic saturation of sintered samples. As shown in the figure, the coercivity decreases with an increase in sintering temperature. The reason is that the WC grains grow as the sintering temperature increases. When the Co content remains constant, the coercivity of WC-10Co cemented carbide decreases with the average WC grain size increase, which is consistent with the inversely proportional relationship between them [54]. The coercive force was mainly concerned with the cobalt content and the dispersion degree of the bonding phase. Generally, if the WC grain is approximately fine, the smaller the binder's mean free path, the higher the coercive force [19]. The magnetic saturation values of cemented carbide alloys at different sintering temperatures fluctuate. The reason is that the redox reaction occurs when the alloy specimen is placed in the air, resulting in the loss of carbon content in the alloy, which leads to fluctuations in the magnetic saturation value, and the degree of a redox reaction is not uniform.

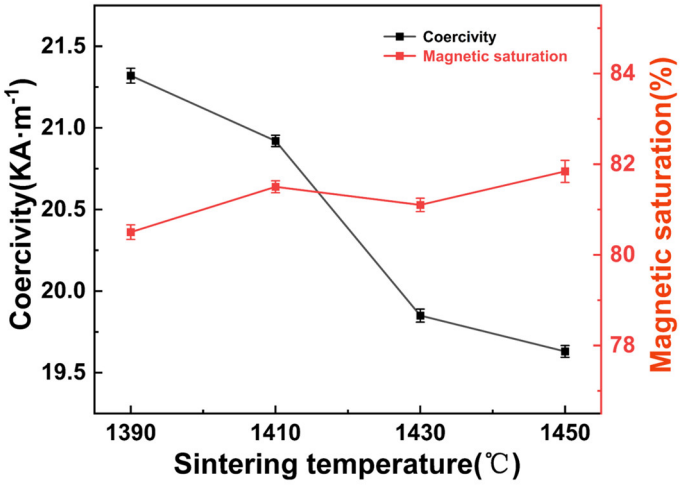

Figure 8. Magnetic properties of the WC-10Co-0.5Cr_3C_2-1TaC-0.5Ru cemented carbide at different sintering temperatures.

3.4. Mechanical Properties

Figure 9 shows the mechanical properties of WC-10 wt.%Co cemented carbide at different sintering temperatures. Hardness and fracture toughness are cemented carbide's two most important mechanical properties. As shown in Figure 9, there is an opposite relationship between hardness and fracture toughness. As the sintering temperature increases, the hardness decreases while the fracture toughness increases. The change in hardness can be explained by the two following aspects. The first is a decrease in porosity and an increase in relative density, which improve hardness [55]. The second is the occurrence of grain growth. As is well known, according to the Hall–Petch relationship, the hardness of an alloy is determined by the WC grain size. The grain size growth will lead to a decrease in hardness [56]. According to the data in Tables 2 and 3, it can be seen that when the temperature increases from 1390 °C to 1410 °C, the pores of the cemented

carbide decrease and the relative density increases, thus increasing the hardness. As the sintering temperature continues to increase, the change is not apparent. From the change in the average grain size of WC shown in Figure 7, it can be seen that as the temperature increases, the WC grains grow, leading to a decrease in hardness. Hardness is related to densification and grain coarsening, which counteract each other, with the latter having a more significant influence [35]. As a result, the change in hardness is less pronounced, but the overall trend is downward. With the increase in sintering temperature, the fracture toughness of sintered samples increased from 13.2 MPa·$m^{1/2}$ to 15.3 MPa·$m^{1/2}$. The reason is that the fracture toughness of alloys is mainly dependent on the WC grain size when the Co content remains constant [24]. The finer the WC grain size of the sintered sample, the lower the fracture toughness, and vice versa [57]. Thus, a rise in sintering temperature will increase grain size, increasing fracture toughness.

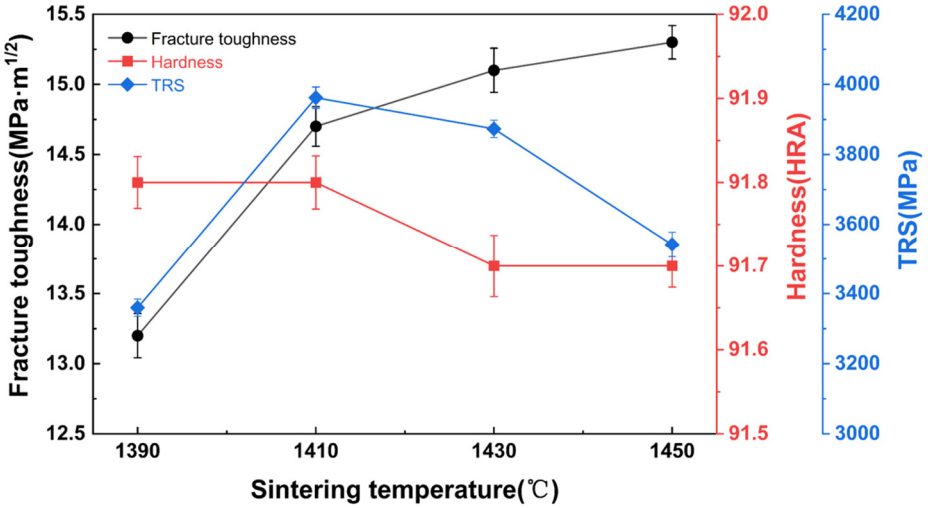

Figure 9. Change in mechanical properties of the WC-10Co-0.5Cr_3C_2-1TaC-0.5Ru cemented carbide at different sintering temperatures.

As shown in Figure 9, TRS shows a tendency to increase and then decrease with increasing sintering temperature. The highest TRS is found for the cemented carbide sintered at 1410 °C, which reaches 3962 MPa. The reason for this is the presence of many Class A pore defects in the alloy sintered at 1390 °C. Fracture sources can easily form at the pores, which can cause an intense build-up of internal stress and nucleate cracks during deformation, thus causing a decrease in the TRS of the alloy [58]. When the sintering temperature increases, the pores decrease, benefiting TRS. However, with the increase in sintering temperature, WC grains grow abnormally, and coarse grains are prone to form fracture sources, thus leading to a decreasing trend in TRS [59]. It has been shown that the TRS of the alloy can be improved by refining the WC grains [60].

4. Conclusions

The study investigated the influence of sintering temperature on the microstructure and properties of fine-grained WC-10Co-0.5Cr_3C_2-1TaC-0.5Ru cemented carbide. The main conclusions can be drawn as follows:

1. When the sintering temperature is below 1410 °C, the porosity of the WC-Co cemented carbide decreases with increasing sintering temperature. At 1410 °C, the alloy achieves a relative density of 99.98% and remains unchanged.
2. The average grain size of the WC-Co cemented carbide increases, and the size distribution becomes broader with the rise in sintering temperature. The coercive force of the cemented carbide decreases with increasing grain size, while the fracture toughness increases.

3. Hardness is influenced by both density and grain coarsening. The hardness of the sintered material increases with increasing density but decreases with larger grain size, showing a decreasing trend due to the combined effect of both factors. The transverse rupture strength (TRS) shows an initial increase and then a decrease with the rise in sintering temperature.
4. At a sintering temperature of 1410 °C, the cemented carbide exhibits excellent mechanical properties. It has the highest relative density (99.98%), the highest hardness of 91.8 HRA, and the highest TRS of 3962 MPa, along with a relatively high fracture toughness of 14.7 MPa·$m^{1/2}$. In summary, 1410 °C is the optimal sintering temperature for preparing fine-grained WC-10Co-0.5Cr_3C_2-1TaC-0.5Ru cemented carbide.

Author Contributions: Conceptualization, Y.H., L.H. and W.F.; Methodology, Y.H., Q.Q., L.H. and W.F.; Validation, Y.H., K.X. and L.Y.; Formal analysis, Y.H., K.X. and L.H.; Investigation, Y.H., Q.Q., L.Y. and L.H.; Resources, L.H. and W.F.; Data curation, Y.H. and L.H.; Writing—original draft, Y.H. and L.H.; Writing—review and editing, Y.H. and L.H.; Visualization, W.F.; Supervision, L.H. and W.F.; Project administration, W.F.; Funding acquisition, L.H. and W.F. All authors have read and agreed to the published version of the manuscript.

Funding: This study was financially supported by the Opening Foundation of Sichuan Province Engineering Technology Research Center of Powder Metallurgy (SC-FMYJ2023-01).

Institutional Review Board Statement: Not applicable.

Informed Consent Statement: Not applicable.

Data Availability Statement: Data are contained within the article.

Conflicts of Interest: The authors declare no conflict of interest.

References

1. Kresse, T.; Meinhard, D.; Bernthaler, T.; Schneider, G. Hardness of WC-Co hard metals: Preparation, quantitative microstructure analysis, structure-property relationship and modelling. *Int. J. Refract. Met. Hard Mater.* **2018**, *75*, 287–293. [CrossRef]
2. Yu, B.; Li, Y.; Lei, Q.; Nie, Y. Microstructures and mechanical properties of WC-Co-xCr-Mo cement carbides. *J. Alloys Compd.* **2019**, *771*, 636–642. [CrossRef]
3. García, J.; Collado Ciprés, V.; Blomqvist, A.; Kaplan, B. Cemented carbide microstructures: A review. *Int. J. Refract. Met. Hard Mater.* **2019**, *80*, 40–68. [CrossRef]
4. Liu, X.; Liu, X.; Lu, H.; Wang, H.; Hou, C.; Song, X.; Nie, Z. Low-energy grain boundaries in WC-Co cemented carbides. *Acta Mater.* **2019**, *175*, 171–181. [CrossRef]
5. Cai, C.; Boyun, H.; Zuming, L.; Yongxia, L.; Dan, Z.; Tao, L.; Yiming, C.; Lei, C. Additive manufacturing of WC-Co cemented carbides: Process, microstructure, and mechanical properties. *Addit. Manuf.* **2023**, *63*, 103410.
6. Yuan, Y.; Fu, L.; Li, J. Annealing effect on the mechanical properties of ultrafine WC–Co materials. *J. Appl. Res. Technol.* **2017**, *15*, 396–401. [CrossRef]
7. Liu, X.; Song, X.; Wang, H.; Hou, C.; Liu, X.; Wang, X. Reinforcement of tungsten carbide grains by nanoprecipitates in cemented carbides. *Nanotechnology* **2016**, *27*, 415710. [CrossRef]
8. Chang, S.-H.; Chang, M.-H.; Huang, K.-T. Study on the sintered characteristics and properties of nanostructured WC–15 wt% (Fe–Ni–Co) and WC–15 wt% Co hard metal alloys. *J. Alloys Compd.* **2015**, *649*, 89–95. [CrossRef]
9. Fabijanić, T.A.; Alar, Ž.; Ćorić, D. Influence of consolidation process and sintering temperature on microstructure and mechanical properties of near nano- and nano-structured WC-Co cemented carbides. *Int. J. Refract. Met. Hard Mater.* **2016**, *54*, 82–89. [CrossRef]
10. Lee, H.C.; Gurland, J. Hardness and deformation of cemented tungsten carbide. *Mater. Sci. Eng.* **1978**, *33*, 125–133. [CrossRef]
11. Jucan, O.-D.; Gădălean, R.-V.; Chicinaș, H.-F.; Bâlc, N.; Popa, C.-O. The Assessment of the Transversal Rupture Strength (TRS) and Hardness of WC-Co Specimens Made via Additive Manufacturing and Sinter-HIP. *Metals* **2023**, *13*, 1051. [CrossRef]
12. Liu, C.; Lin, N.; He, Y.; Wu, C.; Jiang, Y. The effects of micron WC contents on the microstructure and mechanical properties of ultrafine WC–(micron WC–Co) cemented carbides. *J. Alloys Compd.* **2014**, *594*, 76–81. [CrossRef]
13. Emani, S.V.; Wang, C.; Shaw, L.L.; Chen, Z. On the hardness of submicrometer-sized WC–Co materials. *Mater. Sci. Eng. A* **2015**, *628*, 98–103. [CrossRef]
14. Yang, G.-J.; Gao, P.-H.; Li, C.-X.; Li, C.-J. Simultaneous strengthening and toughening effects in WC–(nanoWC–Co). *Scr. Mater.* **2012**, *66*, 777–780. [CrossRef]
15. Fang, Z.Z.; Wang, H.; Kumar, V. Coarsening, densification, and grain growth during sintering of nano-sized powders—A perspective. *Int. J. Refract. Met. Hard Mater.* **2017**, *62*, 110–117. [CrossRef]

16. Lin, H.; Sun, J.; Li, C.; He, H.; Qin, L.; Li, Q. A facile route to synthesize WC–Co nanocomposite powders and properties of sintered bulk. *J. Alloys Compd.* **2016**, *682*, 531–536. [CrossRef]
17. Poetschke, J.; Richter, V.; Gestrich, T.; Michaelis, A. Grain growth during sintering of tungsten carbide ceramics. *Int. J. Refract. Met. Hard Mater.* **2014**, *43*, 309–316. [CrossRef]
18. Chen, H.; Yang, Q.; Yang, J.; Yang, H.; Chen, L.; Ruan, J.; Huang, Q. Effects of VC/Cr_3C_2 on WC grain morphologies and mechanical properties of WC-6wt.%Co cemented carbides. *J. Alloys Compd.* **2017**, *714*, 245–250. [CrossRef]
19. Wu, C.-C.; Chang, S.-H.; Tang, T.-P.; Peng, K.-Y.; Chang, W.-C. Study on the properties of WC-10Co alloys adding Cr_3C_2 powder via various vacuum sintering temperatures. *J. Alloys Compd.* **2016**, *686*, 810–815. [CrossRef]
20. Gao, Y.; Yan, M.-Y.; Luo, B.-H.; Ouyang, S.; Chen, W.; Bai, Z.-H.; Jing, H.-B.; Zhang, W.-W. Effects of NbC additions on the microstructure and properties of non-uniform structure WC-Co cemented carbides. *Mater. Sci. Eng. A* **2017**, *687*, 259–268. [CrossRef]
21. Boccarusso, L.; Scherillo, F.; Prisco, U. Effects of Cr_3C_2 Addition on Wear Behaviour of WC-Co Based Cemented Carbides. *Metals* **2018**, *8*, 895. [CrossRef]
22. Zhang, H.; Xiong, J.; Guo, Z.; Yang, T.; Liu, J.; Hua, T. Microstructure, mechanical properties, and cutting performances of WC-Co cemented carbides with Ru additions. *Ceram. Int.* **2021**, *47*, 26050–26062. [CrossRef]
23. Zhao, C.; Lu, H.; Liu, X.; Liu, C.; Nie, Z.; Song, X. Strengthening cemented carbides by activated nano TaC. *Int. J. Refract. Met. Hard Mater.* **2021**, *95*, 105449. [CrossRef]
24. Yin, C.; Ruan, J.; Du, Y.; Long, J.; Peng, Y.; Li, K. Effects of Cr_3C_2, VC, and TaC on Microstructure, WC Morphology and Mechanical Properties of Ultrafine WC–10 wt. % Co Cemented Carbides. *Metals* **2020**, *10*, 1211. [CrossRef]
25. Rubiano Buitrago, J.D.; Gil Plazas, A.F.; Herrera Quintero, L.K. Influence of TiC and Cr_3C_2 additions on the mechanical properties of a (W-Ti-Cr)C-Co sintered hardmetal. *J. Mater. Res. Technol.* **2019**, *8*, 5736–5744. [CrossRef]
26. Fang, Z.Z.; Wang, X.; Ryu, T.; Hwang, K.S.; Sohn, H.Y. Synthesis, sintering, and mechanical properties of nanocrystalline cemented tungsten carbide—A review. *Int. J. Refract. Met. Hard Mater.* **2009**, *27*, 288–299. [CrossRef]
27. Liu, B.; Kong, D.; Dai, B. Influence of Two-step Sintering Method on Microstructure and Performances of Ultrafine-grained WC-4%Co Cemented Carbide. *Cem Carbide* **2019**, *36*, 406–413.
28. Sun, Q.; Chen, H.; Feng, K.; Wang, H.; Guo, Z.; Xiong, J. Sintering WC-8Co Cemented Carbides at Lower Temperature and Pressure. *Adv. Eng. Sci.* **2013**, *45*, 140–145. [CrossRef]
29. Wang, B.; Jia, J.; Wang, Z.; Yin, Z.; Huang, L.; Yuan, J. Fabrication and performance of graded ultrafine WC–Co cemented carbide tool by one/two-step spark plasma sintering. *Ceram. Int.* **2021**, *47*, 8322–8329. [CrossRef]
30. Zhang, L.; Li, J.; Yi, Y.; Liu, Y.; Lu, B. The Influence of the Characteristics of WC Powders on Sintering Sensitivity of Ultrafine-grained Cemented Carbides. *Cem Carbide* **2020**, *37*, 51–59.
31. Hu, D.; Du, J.; Su, G.; Lu, Z.; Zhang, C.; Kong, X.; Xu, C. Effect of SiC nanowhisker addition on microstructure and mechanical properties of regenerated cemented carbides by low-pressure sintering. *Int. J. Appl. Ceram. Technol.* **2021**, *18*, 1222–1234. [CrossRef]
32. Zhu, G.; Peng, J.; Li, W.; Wang, Q. Study on Vacuum sintering and Low Pressure Sintering of Cemented Carbide. *Tool. Eng.* **2015**, *49*, 31–34.
33. Wei, C.; Song, X.; Fu, J.; Lv, X.; Lu, Q.; Gao, Y.; Wang, H. Effect of sintering technologies on properties of WC-Co cemented carbides. *Mater. Sci. Eng. Powder Metall.* **2012**, *17*, 315–320.
34. Ma, C.; Zhu, Y.; Huang, H.; Cheng, D.; Zhou, B. Composition and phase transformation of WC-Co cemented carbide. *J. Zhejiang Univ. Technol.* **2003**, *31*, 1–6.
35. Qin, Q.; Sun, W.; Luan, D.; Wang, Z. Effect of Sintering Temperature on Properties of Ultrafine YG6 Cemented Carbide. *Hot Work. Technol.* **2016**, *45*, 77–79. [CrossRef]
36. Wei, S.; Wan, Z.; Fu, Q.; Chen, Z. Research on YG8 Carbides Prepared by WC-Co Powder on Regeneration and Mixed Rare Earth Oxide. *Hot Work. Technol.* **2015**, *44*, 55–58+62. [CrossRef]
37. Xie, H.; Xiao, Y.; He, Y.; Feng, P.; Huang, Z. Effects of Sinter-HIP on Microstructure and Properties of Cemented Carbides. *China Tungsten Ind.* **2006**, *21*, 27–31.
38. Tian, H.; Peng, Y.; Du, Y.; Zhang, Y.; Zhang, S.; Zheng, J. Optimization of the mechanical properties of ultra-fine WC-Co-Cr_3C_2 cemented carbides via an approach based on thermodynamic calculations and characterization of the experimental results by the Weibull distribution. *Calphad* **2020**, *70*, 101778. [CrossRef]
39. Chen, G.; Fang, Q.; Zhang, C.; Wang, Z.; Sheng, Z. Effects of Sintering Temperature on Microstructure and Properties of WC-14TiC-8Co Ultrafine Cemented Carbide. *Foundry Technol.* **2017**, *38*, 1670–1673. [CrossRef]
40. Yu, S.; Min, F.; Ying, G.; Noudem, J.G.; Liu, S.; Zhang, J. The grain growth and boundary evolution of extra-coarse-grained cemented carbides by pressureless sintering of ball-milling-mixed WC with Co at different temperature. *Mater. Charact.* **2021**, *180*, 111386. [CrossRef]
41. Liu, Z.; Liang, Y.; Zhong, T.; Guo, Y.; Qin, W.; Tang, C. Effect of WC Powder Carbonization and Milling Time on the Microstructure and Properties of Submicron. *China Tungsten Ind.* **2019**, *34*, 48–53.
42. Li, J.; Shi, Y.; Liu, X.; Jiang, L.; Li, B. Effects of sintering temperatures on performance of WC-6Ni non-magnetic cemented carbide by Sinter-HIP. *Powder Metall. Ind.* **2021**, *31*, 46–50. [CrossRef]
43. Schubert, W.D.; Neumeister, H.; Kinger, G.; Lux, B. Hardness to toughness relationship of fine-grained WC-Co hardmetals. *Int. J. Refract. Met. Hard Mater.* **1998**, *16*, 133–142. [CrossRef]

44. Wei, C.; Song, X.; Fu, J.; Lv, X.; Wang, H.; Gao, Y.; Zhao, S.; Liu, X. Effect of Carbon Addition on Microstructure and Properties of WC–Co Cemented Carbides. *J. Mater. Sci. Technol.* **2012**, *28*, 837–843. [CrossRef]
45. Juhani, K.; Letunovitš, S.; Viljus, M.; Pirso, J.; Joost, R. Recycling of WC-Co hardmetals by oxidation and carbothermal reduction in combination with reactive sintering. *Est. J. Eng.* **2012**, *18*, 127. [CrossRef]
46. Kim, J.; Suh, Y.J.; Kang, I. First-principles calculations of the phase stability and the elastic and mechanical properties of η-phases in the WC–Co system. *J. Alloys Compd.* **2016**, *656*, 213–217. [CrossRef]
47. Ke, Z.; Zheng, Y.; Zhang, G.; Ding, Q.; Zhang, J.; Wu, H.; Xu, X.; Lu, X.; Zhu, X. Microstructure and mechanical properties of dual-grain structured WC-Co cemented carbides. *Ceram. Int.* **2019**, *45*, 21528–21533. [CrossRef]
48. Qin, Q.; Sun, W.; Zhang, W.; Li, J.; Luan, D.; Wang, Z. Effect of Ball Milling Time for Microstructure and Properties of Ultrafine YG6 Cemented Carbide. *Tool. Eng.* **2016**, *50*, 42–45. [CrossRef]
49. Amberg, S.; Doxner, H. Porosity in Cemented Carbide. *Powder Metall.* **2013**, *20*, 1–10. [CrossRef]
50. Li, D.; Liu, Y.; Ye, J.; Chen, X.; Wang, L. The enhancement of the microstructure and mechanical performances of ultrafine WC-Co cemented carbides by optimizing Cr2(C,N) addition and WC particle sizes. *Int. J. Refract. Met. Hard Mater.* **2021**, *97*, 105518. [CrossRef]
51. Wang, Y.; Xiang, F.; Yuan, X.; Yang, B.; Wang, F.; Li, Y. Effects of Processing Parameters on the Microstructure and Mechanical Properties of Nanoscaled WC-10Co Cemented Carbide. *Materials* **2022**, *15*, 4472. [CrossRef] [PubMed]
52. Zhenyun, L.; Jin, D.; Yujing, S.; Guosheng, S.; Chongyan, Z.; Xiangmin, K. Effect of ultrafine WC contents on the microstructures, mechanical properties and wear resistances of regenerated coarse grained WC-10Co cemented carbides. *Int. J. Refract. Met. Hard Mater.* **2021**, *97*, 105516.
53. Sun, L.; Jia, C.; Cao, R.; Lin, C. Effects of Cr_3C_2 additions on the densification, grain growth and properties of ultrafine WC–11Co composites by spark plasma sintering. *Int. J. Refract. Met. Hard Mater.* **2008**, *26*, 357–361. [CrossRef]
54. Sun, Y.; Su, W.; Yang, H.; Ruan, J. Effects of WC particle size on sintering behavior and mechanical properties of coarse grained WC–8Co cemented carbides fabricated by unmilled composite powders. *Ceram. Int.* **2015**, *41*, 14482–14491. [CrossRef]
55. Yang, Q.; Yang, J.; Yang, H.; Ruan, J. The effects of fine WC contents and temperature on the microstructure and mechanical properties of inhomogeneous WC-(fine WC-Co) cemented carbides. *Ceram. Int.* **2016**, *42*, 18100–18107. [CrossRef]
56. Hansen, N. Hall–Petch relation and boundary strengthening. *Scr. Mater.* **2004**, *51*, 801–806. [CrossRef]
57. Chen, J.; Liu, W.; Deng, X.; Wu, S. Effects of Mo and Vc on the microstructure and properties of nano-cemented carbides. *Sci. Sinter.* **2016**, *48*, 41–50. [CrossRef]
58. Shen, T.T.; Xiao, D.H.; Ou, X.Q.; Song, M.; He, Y.H.; Lin, N.; Zhang, D.F. Effects of LaB6 addition on the microstructure and mechanical properties of ultrafine grained WC–10Co alloys. *J. Alloys Compd.* **2011**, *509*, 1236–1243. [CrossRef]
59. Chang, S.-H.; Chang, P.-Y. Study on the mechanical properties, microstructure and corrosion behaviors of nano-WC–Co–Ni–Fe hard materials through HIP and hot-press sintering processes. *Mater. Sci. Eng. A* **2014**, *618*, 56–62. [CrossRef]
60. Lin, T.; Li, Q.; Han, Y.; Song, K.; Wang, X.; Shao, H.; Dong, J.; Wang, H.; Deng, X. Effects of Nb and NbC additives on microstructure and properties of WC-Co-Ni cemented carbides. *Int. J. Refract. Met. Hard Mater.* **2022**, *103*, 105782. [CrossRef]